Pharmaceutical Sciences and Drug Design
ISSN: 3062-4428
2026, Volume 6, Issue 1, Page No: 1-18
Copyright CC BY-NC-SA 4.0
Available online at: www.galaxypub.co/page/journals

Galaxy Publication

Nanoemulsified *Ocotea indecora* Essential Oil: Improved Antifungal and Antimicrobial Performance

Claire Martin[1], Julien Robert[2]*, Sophie Bernard[1], Antoine Girard[2]

[1]Department of Pharmaceutical Chemistry and Drug Design, Faculty of Pharmacy, University of Lyon, Lyon, France.
[2]Department of Applied Drug Discovery, Faculty of Medicine, University of Strasbourg, Strasbourg, France.

***E-mail** ✉ julien.robert@gmail.com

Received: 12 September 2025; **Revised:** 21 December 2025; **Accepted:** 08 January 2026

ABSTRACT

Antimicrobial resistance, along with fungal contamination, continues to pose significant risks to public health and agricultural systems, underscoring the urgent need for novel alternatives. Bioactive compounds derived from plants represent a promising source, and their effectiveness may be further improved through nanoformulation strategies. This work evaluated the antimicrobial activity of *Ocotea indecora* essential oil and its corresponding nanoemulsion. GC-MS analysis of the essential oil identified sesquirosefuran (91.61%) as the dominant compound. An optimized nanoemulsion was developed using a factorial design, producing stable spherical nanodroplets with an average size of 79 nm and a PdI of 0.029, demonstrating long-term stability. The essential oil inhibited both Gram-positive and Gram-negative bacteria at concentrations of 1-2 mg/mL, whereas the nanoemulsion significantly enhanced bactericidal efficacy against *Staphylococcus aureus*. Conversely, antifungal testing showed stronger activity, with the nanoemulsion reducing the minimum inhibitory concentration to 625 µg/mL against *Thielaviopsis ethacetica*, thereby enhancing the antifungal performance of the essential oil (2.5 mg/mL). Microscopic analysis further revealed structural damage, including reduced hyphal thickness and disrupted sporulation, indicating decreased fungal virulence. Overall, *O. indecora* essential oil demonstrates notable antimicrobial properties, and nanoemulsification was particularly effective in enhancing antifungal activity, with only modest improvements in antibacterial activity. These findings highlight *O. indecora* derivatives as promising natural resources for the development of new antimicrobial therapies.

Keywords: *Thielaviopsis ethacetica*, Antibacterial, Antifungal, Lauraceae, *Staphylococcus aureus*

How to Cite This Article: Martin C, Robert J, Bernard S, Girard A. Nanoemulsified *Ocotea indecora* Essential Oil: Improved Antifungal and Antimicrobial Performance. Pharm Sci Drug Des. 2026;6(1):1-18. https://doi.org/10.51847/ppM2BoPmgu

Introduction

Bacterial and fungal organisms pose serious threats to human health and agriculture, as they act as infectious agents, produce toxins, and contaminate food products [1]. Hospital-acquired infections remain particularly problematic in clinical environments, especially among neonates and patients in intensive care units, who are more susceptible due to their weakened condition and exposure to invasive medical procedures [2]. Members of the ESKAPE group, including *Enterococcus faecium*, *Staphylococcus aureus*, *Klebsiella pneumoniae*, *Acinetobacter baumannii*, *Pseudomonas aeruginosa*, and *Enterobacter* spp., are characterized by pronounced antimicrobial resistance, thereby limiting therapeutic options and complicating clinical management [3]. Similarly, fungi contribute substantially to global health and economic challenges through their roles in infectious diseases, mycotoxin production, and post-harvest spoilage of agricultural products, underscoring the critical need for innovative preventive and control strategies [1, 4].

The evolutionary adaptation of bacteria and fungi under natural selection has contributed significantly to the development of resistance against antimicrobial agents and phytosanitary compounds [5, 6]. In bacterial populations, inappropriate antibiotic use, self-medication practices, insufficient therapeutic regimens, and

© 2026 Pharmaceutical Sciences and Drug Design

diagnostic delays have collectively increased reliance on broad-spectrum antibiotics, thereby accelerating the emergence of resistance [6]. In parallel, fungal organisms have also developed resistance, a process further intensified by the long-term and repetitive application of identical agrochemical agents in agricultural systems [5]. A notable phytopathogen affecting tropical crops such as pineapple, coconut, banana, sugarcane, and oil palm is *Thielaviopsis ethacetica* Went., which corresponds to the anamorphic stage of *Ceratocystis paradoxa* (Dade) C. Moreau [7, 8]. This situation underscores the urgent need for innovative antimicrobial and phytosanitary solutions that are both safe and environmentally compatible, to address the increasing resistance observed in clinically relevant bacterial pathogens and fungal agents responsible for substantial agricultural losses worldwide [4, 9, 10].

Together, these issues highlight the urgent need for alternative strategies that can mitigate microbial contamination and infectious diseases while preserving human health, food security, and environmental integrity [11]. Although conventional control approaches predominantly depend on synthetic pesticides and chemical additives, their associated adverse effects on human health, non-target organisms, and ecosystems have raised increasing global concern [12, 13]. In this context, natural products are considered promising alternatives due to their chemical diversity and potentially reduced ecological toxicity [14]. Among them, essential oils are complex mixtures of secondary metabolites that exhibit antimicrobial properties, acting through mechanisms such as disruption of cellular and mitochondrial membranes, disturbance of ion transport processes, and modulation of membrane-associated receptors and proteins [15-17].

Essential oils may also be incorporated into advanced biotechnological systems to enhance their biological performance. In this regard, oil-in-water nanoemulsions have emerged as effective delivery platforms, consisting of oil droplets dispersed in a continuous aqueous phase, typically 20-200 nm in diameter [18]. These nanosystems provide improved physicochemical stability over time and significantly increase the solubility and dispersion of hydrophobic bioactive constituents [19]. Such enhanced dispersion promotes more efficient interactions between plant-derived compounds and microbial targets, ultimately improving antimicrobial efficacy [20].

Ocotea indecora (Shott) Mez (Lauraceae) is a neotropical species endemic to Brazil, commonly known as "canela-sassafrás" in northern Rio de Janeiro. Prior chemical investigations have identified sesquirosefuran as the predominant sesquiterpenoid in the essential oil extracted from leaves collected in this region [21, 22]. The biological activity of the leaf essential oil has been previously documented, including acaricidal effects against *Rhipicephalus (Boophilus) microplus* [21] and insecticidal activity against *Aedes aegypti*, *Drosophila suzukii*, and *Dysdercus peruvianus* [22-24]. Regarding antimicrobial properties, only one prior study has reported fungistatic activity against *Aspergillus* species [25]. Accordingly, the present work offers an expanded evaluation of the antibacterial and antifungal properties of *O. indecora* essential oil and its oil-in-water nanoemulsion, broadening current understanding of its antimicrobial spectrum. By assessing its effects on clinically important bacterial strains and agriculturally relevant fungal pathogens, this study aims to position *O. indecora* as a promising natural source of bioactive metabolites and to determine whether nanoemulsion-based delivery enhances its stability and antimicrobial performance.

Materials and Methods

Plant material

All research activities involving *O. indecora* were registered under SisGen (A491A56) and SisBio/ICMBio (13659-21). Leaf samples were collected from the Restinga de Jurubatiba National Park (22°12.683′ S, 41°35.283′ O), Carapebus, Rio de Janeiro, Brazil. Botanical authentication was performed, and a voucher specimen was prepared and deposited in the herbarium of the University of the State of Rio de Janeiro (UERJ), São Gonçalo, Rio de Janeiro, Brazil, under code RFFP: 16.873.

Essential oil extraction

The essential oil was obtained following the protocol described by Pinto *et al*. [25]. Leaves of *O. indecora* (581 g), previously separated from stems, were mechanically macerated with 3 L of distilled water using a blender (SPL-052, Spolu-benesse, Itajobi, SP, Brazil). The homogenized mixture was transferred to a 5 L round-bottom flask and hydrodistilled for 3 h using a Clevenger-type apparatus. The resulting oil phase was dried with anhydrous sodium sulfate (Na_2SO_4, ≥ 99%, Sigma-Aldrich, St. Louis, MO, USA) and stored at −20 °C in amber borosilicate vials sealed with polypropylene caps.

Essential oil characterization

The essential oil composition was analyzed according to the procedure of Machado *et al*. [26], employing two chromatographic systems: a GC-MS QP2010 (Shimadzu, Kyoto, Japan) for compound identification and a GC-2014 (Shimadzu, Kyoto, Japan) equipped with a flame ionization detector (FID) for quantification of relative abundance. For analysis, 1 µL of the sample diluted in dichloromethane (1000 ppm, ≥ 99.9%, Sigma-Aldrich, St. Louis, MO, USA) was injected at an injector temperature of 260 °C. Helium served as the carrier gas at 1 mL/min, with a split ratio of 1:20. The temperature program began at 60 °C and increased to 290 °C at 3 °C/min. Separation was achieved using an RTX5 MS column (Restek Corporation, Bellefonte, PA, USA; 30 m × 0.25 mm ID × 0.25 µm film thickness). Mass spectrometric detection was performed under electron ionization at 70 eV with a scan rate of 1 scan/s. The FID detector was maintained at 290 °C.

Retention indices (arithmetic index, AI) were calculated using a homologous series of n-alkanes (C7–C40) analyzed under identical chromatographic conditions. Compound assignment was performed by comparing AI values and mass spectra with published literature data [27, 28], supplemented by matching fragmentation patterns with the NIST library. Quantification of constituents was performed using GC-FID under identical analytical conditions to GC-MS, with relative percentages calculated by normalizing peak areas.

Nanoemulsion preparation and characterization

Nanoemulsion formulations were produced following Betzler *et al*. [29], using *O. indecora* essential oil as the oil phase (2–10%, w/w) and Pluronic L-64® (Sigma-Aldrich, St. Louis, MO, USA) as the surfactant phase (10%–15%, w/w). Initially, the oil phase was incorporated dropwise into the aqueous surfactant solution and mixed for 1 min using a vortex mixer (KASVI®, São José dos Pinhais, PR, Brazil; K40-1010). The pre-emulsion was then subjected to ultrasonic homogenization using a UP100H Ultrasonic Processor (Hielscher®, Teltow, BB, Germany) at cycle 1 with amplitudes ranging from 20 to 100 for 1 min. All emulsification steps were carried out in an ice bath to minimize thermal effects.

Before analysis, samples were diluted 1:20 in distilled water and characterized at 25 °C using Dynamic Light Scattering (DLS) with a Nanosizer Nano® S90 (Malvern, UK). Measurements included mean droplet size and polydispersity index (PdI), and all experiments were performed in triplicate.

Experimental design 23

A 2^3 factorial design based on Betzler *et al*. [29] was applied using Statistica 12 software to investigate the effects of three independent variables: sonication amplitude (20–100), essential oil concentration (2%–10%, w/w), and Pluronic L-64 concentration (10%–15%, w/w). The response variables evaluated were mean droplet size (nm) and polydispersity index (PdI), to optimize nanoemulsion formation conditions.

Model adequacy was evaluated through curvature testing, and statistical interpretation was based on the adjusted model. The optimized formulation (Ne-OiEO) was subsequently selected for morphological evaluation using transmission electron microscopy (TEM; Morgagni 268, FEI, Hillsboro, OR, USA). For sample preparation, the nanoemulsion was diluted 1:1 with deionized water, and 5 µL was deposited onto a formvar-coated copper grid. The grid was dried for 1 h in a desiccator before TEM imaging.

Nanoemulsion stability

The optimized nanoemulsion (Ne-OiEO) was prepared in triplicate and stored in amber borosilicate glass vials (5 mL) with black polypropylene screw caps. Stability was evaluated under three storage conditions: ambient temperature (25 °C), refrigeration (8 °C), and accelerated aging in a climatic chamber (42 °C).

Physicochemical stability was monitored by DLS at predefined intervals: 0, 7, 15, 30, 60, and 90 days post-preparation. Parameters analyzed included mean droplet diameter (nm) and polydispersity index (PdI). In parallel, macroscopic stability was assessed visually, including evaluation of color changes, phase separation, creaming, sedimentation, and precipitation throughout the storage period.

Bacterial and fungal strains

The bacterial collection used in this work originated from the Laboratory of Molecular Epidemiology and Biotechnology (LEMB), Fluminense Federal University (Niterói, Rio de Janeiro, Brazil). The panel comprised *Staphylococcus aureus* ATCC 25923 and USA 300, *Staphylococcus epidermidis* ATCC 122282, *Escherichia coli* ATCC 25922, *Enterobacter cloacae* ATCC 13047, *Pseudomonas aeruginosa* ATCC 27853, and *Klebsiella*

pneumoniae ATCC 13883. These strains were preserved in Brain Heart Infusion (BHI) broth containing 10% glycerol and maintained at −80 °C. The fungal isolate *T. ethacetica* E-748 was obtained from the Mycological Collection of the Instituto Capixaba de Pesquisa, Assistência Técnica e Extensão Rural (INCAPER, Espírito Santo, Brazil), with formal registration under SISGEN (AAA459F).

Antibacterial evaluation

MIC were determined in triplicate using the broth microdilution technique in accordance with CLSI standard M07-A10. Bacterial cultures were first streaked on Mueller–Hinton Agar (MHA) and incubated for 24 h to obtain fresh colonies. These colonies were then transferred into 0.85% NaCl solution and adjusted to match a 0.5 McFarland turbidity standard.

For testing, *O. indecora* essential oil was dissolved in 1% DMSO and diluted in 96-well plates containing Mueller–Hinton Broth (MHB), producing concentrations from 2 mg/mL down to 0.015 mg/mL. Control conditions included a blank nanoemulsion (without active oil) and DMSO alone. Vancomycin and ciprofloxacin were used as reference antibiotics for Gram-positive and Gram-negative bacteria, respectively. Incubation was performed at 37 °C for 24 h, after which 20 µL of resazurin indicator was added to visualize bacterial viability.

To determine MBC values, 10 µL aliquots from wells showing no visible growth were transferred onto MHB agar plates divided according to concentration levels. Following a second incubation at 37 °C for 24 h, the MBC was defined as the lowest concentration that showed complete absence of colony formation, corresponding to a 99.9% reduction in bacterial count.

Antifungal evaluation

The antifungal assay against *T. ethacetica* followed the microdilution methodology described by Souza *et al*. (2020) [30] Experiments were performed in sterile 96-well plates containing 100 µL of double-strength Sabouraud Dextrose Broth (SDB) and 100 µL of each treatment solution, in duplicate.

A range of serial concentrations was prepared: 2500–19.53 µg/mL for *O. indecora* essential oil nanoemulsion (Ne-OiEO) and its blank formulation (C-Ne); 10,000–78 µg/mL for *O. indecora* essential oil (OiEO) solubilized in Tween 80; 242–1.8 µg/mL for Tween 80 control (C-EO); and 10–0.07 µg/mL for itraconazole as the positive control. Each well was inoculated with 10 µL of fungal suspension (1×10^6 conidia/mL). Fungal growth controls contained only SDB with inoculum, while sterility controls consisted of SDB with sterile water. Additional plates without inoculum were included to measure background absorbance from each treatment. All plates were incubated in darkness at 25 °C for 90 h.

Fungal proliferation was quantified by measuring absorbance at 630 nm using an automated microplate reader (Thermo Plate Reader, Pittsburgh, PA, USA). After incubation, absorbance data were used to calculate percentage growth inhibition using Eq. 1.

$$\text{Fungal inhibition (\%)} = 100 - \frac{100 \times (A_{630}\ \text{of treated well} - \text{Average } A_{630}\ \text{of treatment background absorption})}{(A_{630}\ \text{of growth well} - \text{Average } A_{630}\ \text{of medium background absorption})} \quad (1)$$

Dose–response relationships were constructed by plotting normalized inhibition percentages against log10-transformed concentrations (µg/mL, w/v). Essential oil-containing treatments and itraconazole were fitted using a nonlinear regression model (Eq. 2), whereas solvent controls followed a linear regression approach (Eq. 3). The sigmoidal model incorporated a variable-slope parameter (Hill coefficient, As) to describe the response behavior. IC50 and As values were estimated using the Levenberg–Marquardt algorithm within GraphPad Prism v.9.0 (GraphPad Software, San Diego, CA, USA).

$$Y = \frac{(100)}{1 + 10^{[log(IC_{50} - X) \times As]}} \quad (2)$$

$$Y = mx + b \quad (3)$$

The MIC was defined as the lowest concentration that prevented visible fungal growth across four replicates and corresponded to at least 80% inhibition on the dose–response curve. From these wells, 10 µL aliquots were transferred onto potato dextrose agar (PDA) plates and incubated at 25 °C for 50 h under a 12 h light/dark cycle. Following transfer, 30 µL of resazurin was added to assess metabolic viability, indicated by a color shift from

purple to pink. The Minimum Fungicidal Concentration (MFC) was defined as the lowest concentration at which no colony growth and no metabolic activity were detected. All experiments were conducted in triplicate.

Microculture method based on poisoned media

To evaluate morphological alterations induced by exposure to natural and synthetic compounds, a modified slide-based microculture technique was employed, allowing visualization of fungal structural changes after treatment uptake. Sterile PDA blocks (6 mm × 6 mm) were positioned at both ends of a sterile support. Each block was treated with 30 µL of the following formulations: nanoemulsion of *O. indecora* essential oil at 2500 µg/mL (C1-Ne-OiEO) and 312 µg/mL (C4-e-OiEO); *O. indecora* essential oil at 10,000 µg/mL (C1-OiOE) and 1250 µg/mL (C4-OiOE); blank nanoemulsion (C-Ne, 2500 µg/mL); Tween 80 (C-EO, 242 µg/mL); and itraconazole (Itra, 10 µg/mL).

After a short equilibration period of 10 min, fungal inoculum (10 µL; 7×10^6 conidia/mL) was deposited along the edges of both treated and control agar surfaces. Coverslips sterilized in advance were placed over each agar segment to provide a surface for fungal attachment and growth. Humidity was maintained by adding 10 mL of sterile distilled water onto sterile gauze positioned along the sides of each Petri dish, effectively creating a sealed, moist chamber (a second 10 mL addition of sterile water was also applied over the gauze). Plates were then sealed and incubated at 25 °C for 96 h under a 12 h light:12 h dark cycle.

At the end of incubation, fungal development was halted by adding 2 mL of formaldehyde to the gauze in each plate, thereby fixing the biological structures for microscopic evaluation. Slides were subsequently examined under an Olympus BX43 microscope using 10×, 20×, and 40× objectives, coupled with a QColor 3 imaging system (Olympus America Inc., Tokyo, Japan). Morphometric measurements were extracted from captured images using ImageJ software version 1.52a [31].

Beyond descriptive microscopy based on Mbenoun *et al*. [32], quantitative morphometric parameters were also recorded, including secondary conidia length and width (n = 30), aleurioconidia length and width (n = 20), and vegetative hyphal width (n = 20) [32]. Because conidia exhibit an ovoid geometry, surface area (µm²) for both secondary conidia and aleurioconidia was calculated using Eq. 4.

$$A_o\ (\mu m^2) = \pi \times \frac{\text{length}\ (\mu m)}{2} \times \frac{\text{width}\ (\mu m)}{2} \quad (4)$$

For statistical analysis, all datasets were processed in GraphPad Prism v.9.0. Normality of distribution was assessed using the Kolmogorov–Smirnov (n = 30) and D'Agostino–Pearson (n > 30) tests, with significance defined at $P < 0.05$. Parametric comparisons were performed using ANOVA, while non-parametric datasets were analyzed using the Kruskal–Wallis test followed by appropriate post hoc testing ($P < 0.05$). The entire experimental workflow was conducted in independent duplicate assays.

Results and Discussion

Essential oil characterization

The essential oil (yield: 0.64%, w/w) was analyzed by GC-MS, which enabled the tentative identification of four chemical constituents **(Figure 1)**, collectively representing 96.29% of the *O. indecora* essential oil composition **(Table 1)**. The major constituent was the sesquiterpene sesquirosefuran (91.61%), followed by β-farnesene (2.95%).

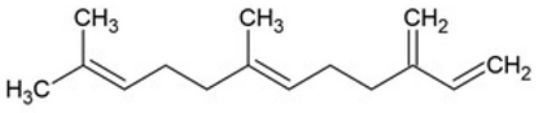

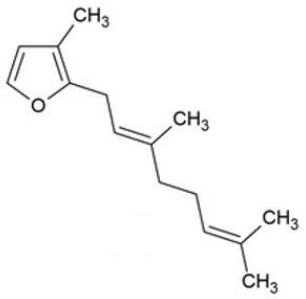

1 2

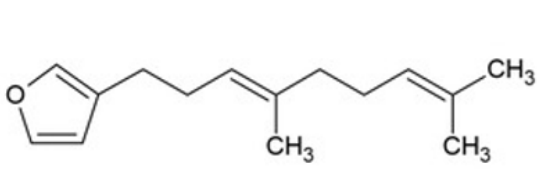

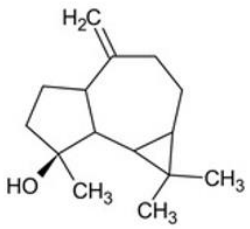

3 4

Figure 1. Chemical constituents of *O. indecora* essential oil: (1) β-farnesene; (2) sesquirosefuran; (3) dendrolasin; and (4) spathulenol.

Table 1. GC-MS and GC-FID profiling of *O. indecora* essential oil obtained from fresh leaves.

Peak	Retention time (RT, min)	AI (Rep)	AI (Library)	Identified compounds	Relative abundance (%)
1	25.485	1265	1454	β-farnesene	2.95
2	29.309	1554	1549	Sesquirosefuran	91.61
3	30.094	1574	1570	Dendrolasin	0.84
4	30.219	1578	1577	Spathulenol	0.89
	TOTAL				96.29
	Sesquiterpene hydrocarbons				2.95
	Oxygenated sesquiterpenes				93.34

Abbreviations: RT = retention time; AIrep = reported arithmetic index; AILit = arithmetic index from Adams (2007) or El-sayed (2025).

Experimental design

The experimental design matrix and responses from the 2^3 factorial setup are summarized in **Table 2**. All formulations produced droplet sizes between 72 and 198.5 nm, while polydispersity index (PdI) values ranged from 0.029 to 0.287 after preparation. The droplet size distribution profiles are presented in **Figure 2**. Formulations 1–3, 5, and 7–11 showed single-peaked (monomodal) distributions, whereas formulations 4 and 6 exhibited dual-peaked (bimodal) behavior.

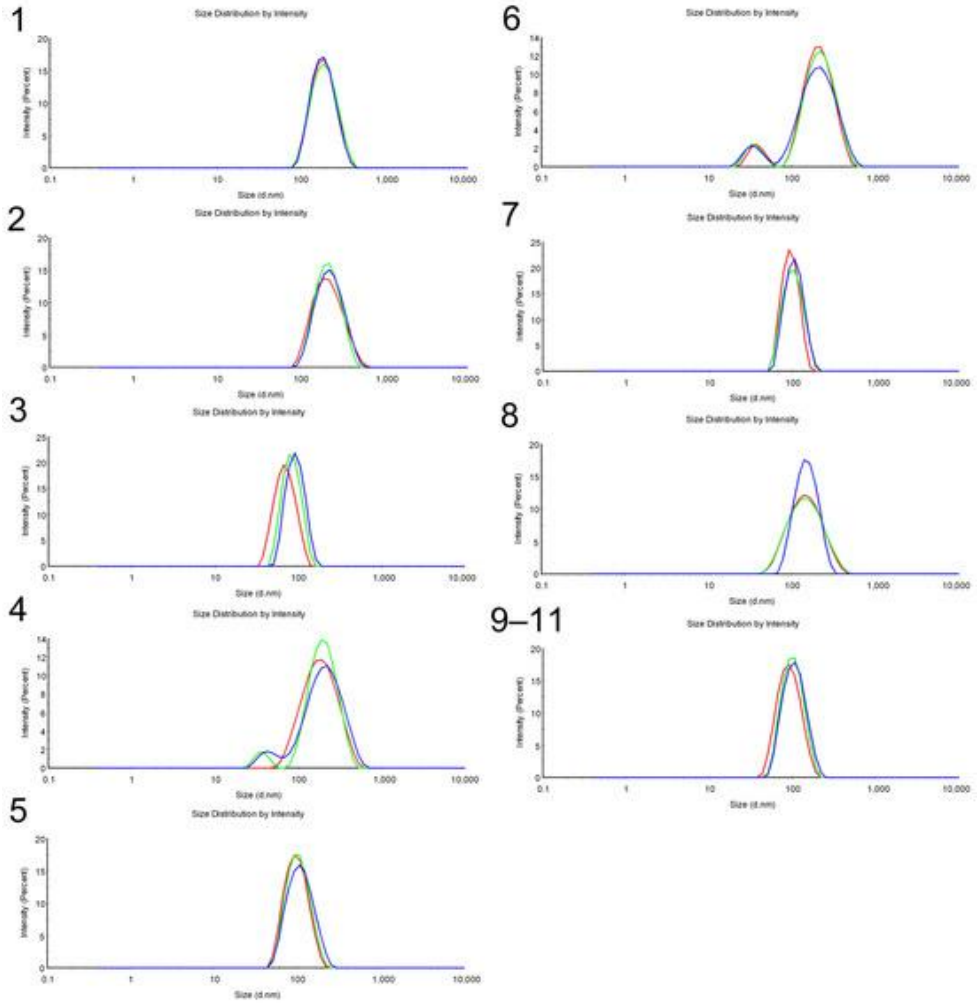

Figure 2. Intensity-based droplet size distribution of nanoformulations 1 to 11. Blue, red, and green curves correspond to three independent replicates (n = 3) from DLS analysis for formulations 1–8, confirming reproducibility. Formulations 9–11 represent center-point replicates of the design, with averaged distributions shown in red (9), green (10), and blue (11).

Table 2. Mean droplet diameter (nm) and polydispersity index of *O. indecora* formulations.

Formulation	Polydispersity index	Mean droplet diameter (nm)	Independent formulation variables C	Independent formulation variables B	Independent formulation variables A
1	0.107 ± 0.015	178.0 ± 2.8	20.0	10.0	2.0
2	0.121 ± 0.018	198.5 ± 3.0	20.0	10.0	10.0
3	0.045 ± 0.020	79.1 ± 11.8	20.0	15.0	2.0
4	0.248 ± 0.017	157.5 ± 2.2	20.0	15.0	10.0
5	0.205 ± 0.033	109.8 ± 5.8	100.0	10.0	2.0
6	0.287 ± 0.026	151.0 ± 3.6	100.0	10.0	10.0
7	0.029 ± 0.021	72.0 ± 10.4	100.0	15.0	2.0
8	0.208 ± 0.012	136.3 ± 2.0	100.0	15.0	10.0
9	0.122 ± 0.020	108.6 ± 6.1	60.0	12.5	6.0
10	0.081 ± 0.010	90.55 ± 9.4	60.0	12.5	6.0
11	0.077 ± 0.012	94.45 ± 7.0	60.0	12.5	6.0

A, essential oil (%, w/w); B, Pluronic-L64 (%, w/w); C, sonication amplitude.

The 2^3 factorial design, including curvature evaluation and pure-error analysis, indicated that all independent variables (oil content, Pluronic L64 concentration, and sonication amplitude) significantly influenced droplet size ($P < 0.05$), with strong model performance ($R^2 = 0.98$; adjusted $R^2 = 0.94$). For PdI, significant effects were

observed for oil concentration (P = 0.021) and its interaction with amplitude (P = 0.045) **(Figure 3)**. The absence of a significant lack-of-fit confirmed that the models adequately represented the experimental behavior. These findings demonstrate that all studied factors contribute to droplet size variation, whereas PdI is mainly governed by oil concentration with additional interaction effects (BC), reflecting complex nonlinear formulation behavior.

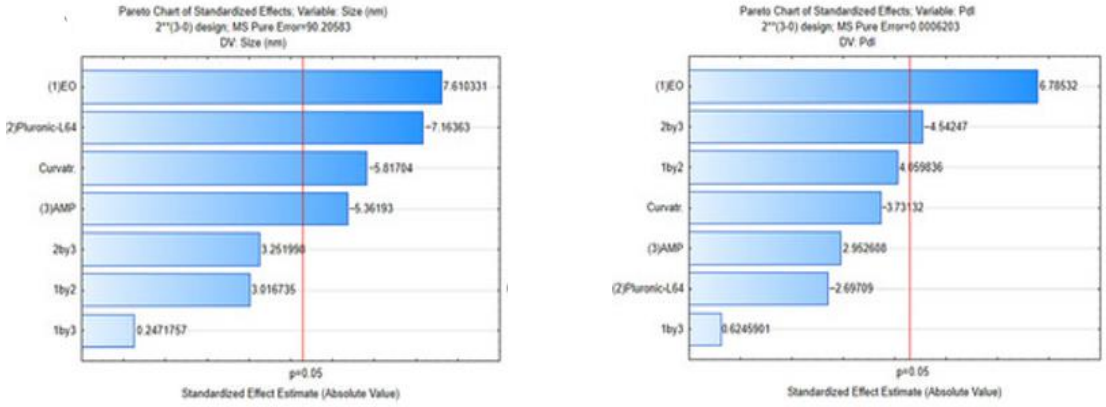

a) b)

Figure 3. Standardized Pareto charts showing factor effects in the 2^3 design on (a) droplet size and (b) polydispersity index (PdI) of *O. indecora* nanoemulsions. The vertical line indicates statistical significance ($P < 0.05$).

Response surface analysis revealed clear trends in both responses **(Figure 4)**. Minimum droplet sizes were obtained under conditions combining low oil content, high Pluronic L64 concentration, and high sonication amplitude, indicating synergistic interactions between formulation and processing parameters **(Figures 4a–4c)**. For PdI, reduced values were mainly associated with lower oil concentration, while the combined effects of surfactant level and amplitude further improved size uniformity **(Figures 4d–4f)**. Overall, optimal nanoemulsion properties were achieved at 2% oil, 15% surfactant, and 100% sonication amplitude.

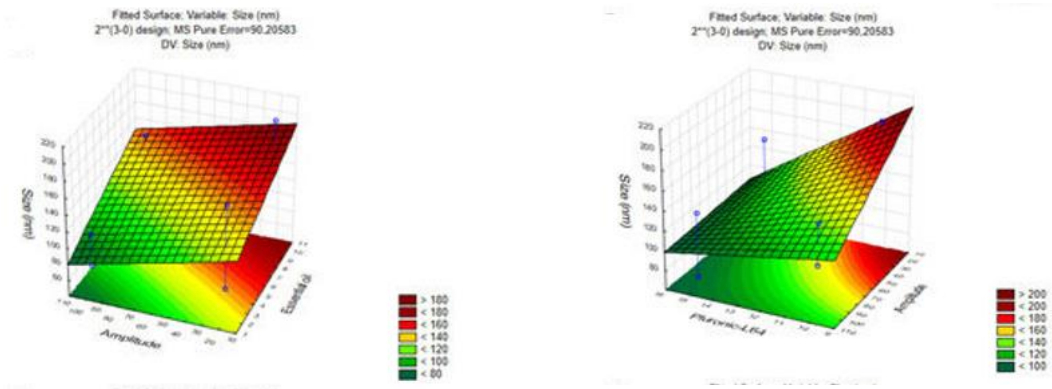

a) b)

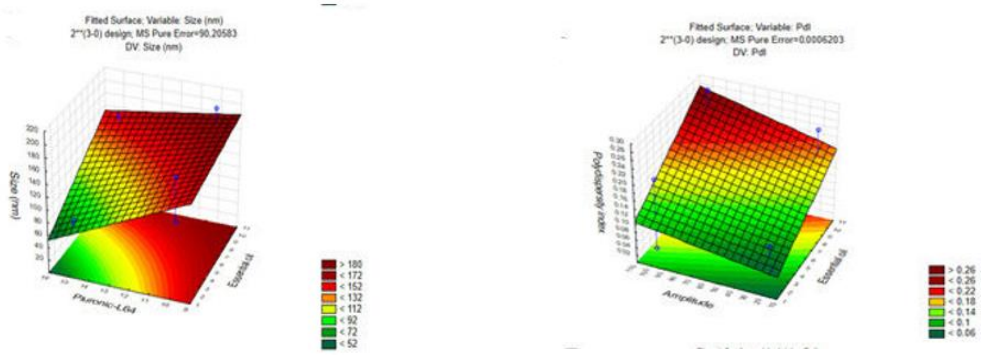

c) d)

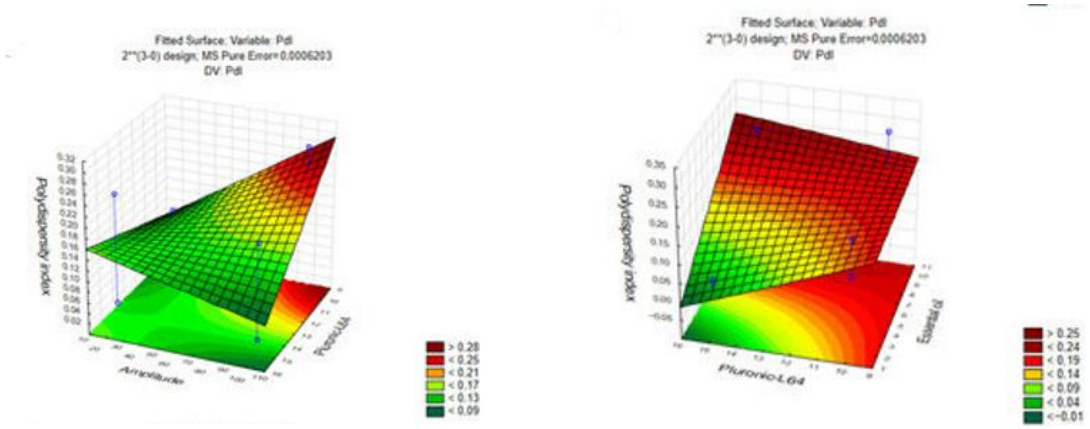

e) f)

Figure 4. Three-dimensional response surface plots for *O. indecora* nanoemulsions. Panels (a–c) depict droplet size responses: (a) amplitude × oil, (b) Pluronic L64 × amplitude, (c) Pluronic L64 × oil. Panels (D–F) show PdI responses under the same variable combinations. The third factor was fixed at its central level (oil = 6%, Pluronic L64 = 12.5%, amplitude = 60).

Based on optimization results, the selected nanoemulsion (Ne-OiOE; 2% EO, 15% Pluronic L-64, amplitude 100) was analyzed using transmission electron microscopy (TEM). At 89,000× magnification, spherical nanodroplets predominantly below 120 nm were observed, consistent with DLS measurements. The morphology appeared uniform, supporting the low PdI values (0.029 ± 0.021) **(Figure 5).**

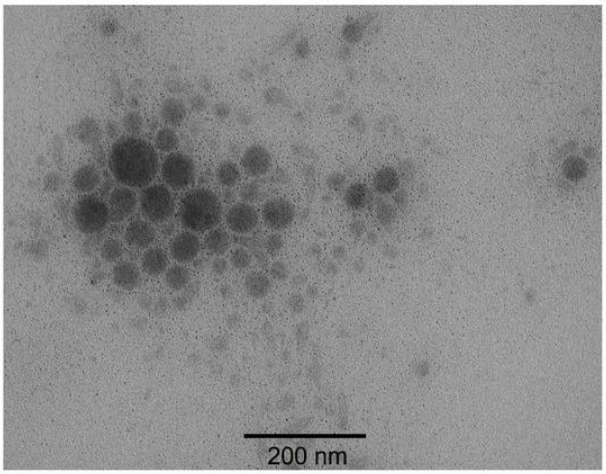

Figure 5. TEM micrographs of *O. indecora* essential oil nanoemulsion (Ne-OiOE) droplets.

Nanoemulsion stability

At room temperature (25 ± 2 °C), the Ne-OiOE formulation maintained colloidal stability for 90 days, remaining visually transparent with a slight bluish hue. Its droplet size distribution remained within 76.56–104 nm, and PdI values remained low (0.015–0.058), as summarized in **Table 3**. When stored under refrigeration (8 ± 2 °C), the system became more opaque, developed a milky appearance, and showed increased viscosity over time. This behavior is consistent with the thermoresponsive nature of the Pluronic L-64 surfactant system. To maintain measurement consistency, refrigerated samples were equilibrated to 25 °C before DLS analysis to restore their original transparent blue appearance before evaluation. Under these conditions, the formulation remained overall stable for 90 days; however, statistically significant increases in droplet size (78.36–130 nm, $P < 0.0001$) and PdI (0.020–0.210, $P < 0.0001$) were observed. In contrast, samples kept at elevated temperature in a climatic chamber (40 ± 2 °C) showed clear instability, including phase separation (creaming) after 30 days and a continuous increase in both droplet size and PdI over time ($P < 0.0001$).

Table 3. Stability behavior of *O. indecora* nanoemulsion (Ne-OiOE) during 90 days of storage at 25 °C, 8 °C, and 40 °C conditions.

Storage time (days)	40 ± 2 °C (PdI)	40 ± 2 °C (Size, nm)	8 ± 2 °C (PdI)	8 ± 2 °C (Size, nm)	25 ± 2 °C (PdI)	25 ± 2 °C (Size, nm)
0	0.042 ± 0.008	81.05 ± 10.53	0.020 ± 0.005	78.36 ± 7.99	0.015 ± 0.010	76.56 ± 11.76
7	0.145 ± 0.023 f	131.3 ± 5.76 e	0.055 ± 0.019	85.20 ± 8.86	0.032 ± 0.011 b	83.46 ± 08.79
14	0.119 ± 0.010 f	96.83 ± 6.54	0.107 ± 0.013 d	79.11 ± 12.30	0.054 ± 0.017	80.15 ± 10.50
21	0.154 ± 0.025 f	131.0 ± 6.01 e	0.023 ± 0.004	79.20 ± 10.10	0.051 ± 0.014	73.06 ± 09.82
30	0.230 ± 0.047 f	199.6 ± 1.81 e	0.034 ± 0.009	73.11 ± 10.28	0.056 ± 0.020	72.36 ± 09.88
60	0.161 ± 0.021 f	128.8 ± 5.30 e	0.048 ± 0.014	94.84 ± 11.57	0.051 ± 0.013	104.00 ± 04.63 a
90	0.146 ± 0.040 f	135.9 ± 11.65 e	0.210 ± 0.023 d	122.1 ± 13.11 c	0.058 ± 0.012	71.81 ± 12.26

a ($P = 0.0149$); b ($P < 0.0003$); c ($P < 0.0001$); d ($P < 0.0001$); e ($P < 0.0001$); f ($P < 0.0001$).

Antibacterial assay

The antibacterial performance of both the essential oil and its nanoemulsion was assessed through MIC determination using a microdilution method **(Table 4)**. No inhibitory activity was detected against Gram-negative strains (*E. coli*, *E. cloacae*, *P. aeruginosa*, and *K. pneumoniae*) at the maximum tested concentration of 2 mg/mL for either formulation. In contrast, Gram-positive bacteria were inhibited up to 2048 µg/mL, except for methicillin-sensitive Staphylococcus aureus (MSSA, ATCC 25923), which was inhibited at 1024 µg/mL by both the essential oil and the nanoemulsion. Notably, the nanoemulsion showed a lower bactericidal endpoint (1024 µg/mL) than the essential oil (2048 µg/mL). As reference controls, vancomycin inhibited Gram-positive strains at 1 µg/mL, while ciprofloxacin showed activity below 3.9 µg/mL against Gram-negative organisms. Neither the blank nanoemulsion nor the DMSO control (1%) exhibited antibacterial effects.

Table 4. MIC and MBC values (µg/mL) of *O. indecora* essential oil (OiEO) and nanoemulsion (Ne-OiOE) against bacterial strains.

Microbial strains	Ne-OiEO (MBC)	Ne-OiEO (MIC)	OiEO (MBC)	OiEO (MIC)
***Staphylococcus aureus* ATCC 25923 (MSSA)**	1024	1024	2048	1024
***Staphylococcus aureus* USA300 (MRSA)**	2048	2048	2048	2048
***Staphylococcus epidermidis* ATCC 122282**	2048	048	2048	2048
***Escherichia coli* ATCC 25922**	> 2048	> 2048	> 2048	> 2048
***Enterobacter cloacae* ATCC 13047**	>2048	> 2048	> 2048	> 2048
***Pseudomonas aeruginosa* ATCC 27853**	> 2048	> 2048	> 2048	> 2048
***Klebsiella pneumoniae* ATCC 13883**	> 2048	> 2048	> 2048	> 2048

Antifungal assays

Fungistatic activity

Antifungal activity of the essential oil (OiEO) and nanoemulsion (Ne-OiEO) was examined using a quantitative microdilution approach at different concentrations. After 90 h of incubation, fungal growth was evident in all wells containing fungal blank (FB) and negative controls (Tween 80, C-EO, and blank nanoemulsion C-Ne). In contrast, no growth was observed in wells treated with OiEO, Ne-OiEO, or itraconazole. The inhibitory response of *T. ethacetica* was further evaluated using dose–response modeling based on vegetative growth suppression **(Figure 6)**. Inhibition percentages were calculated by comparing the absorbance values of treated wells with those of fungal controls under identical conditions. Variability between experimental plates was observed across all treatments, with the strongest reduction in absorbance recorded for the nanoemulsion (Ne-OiEO).

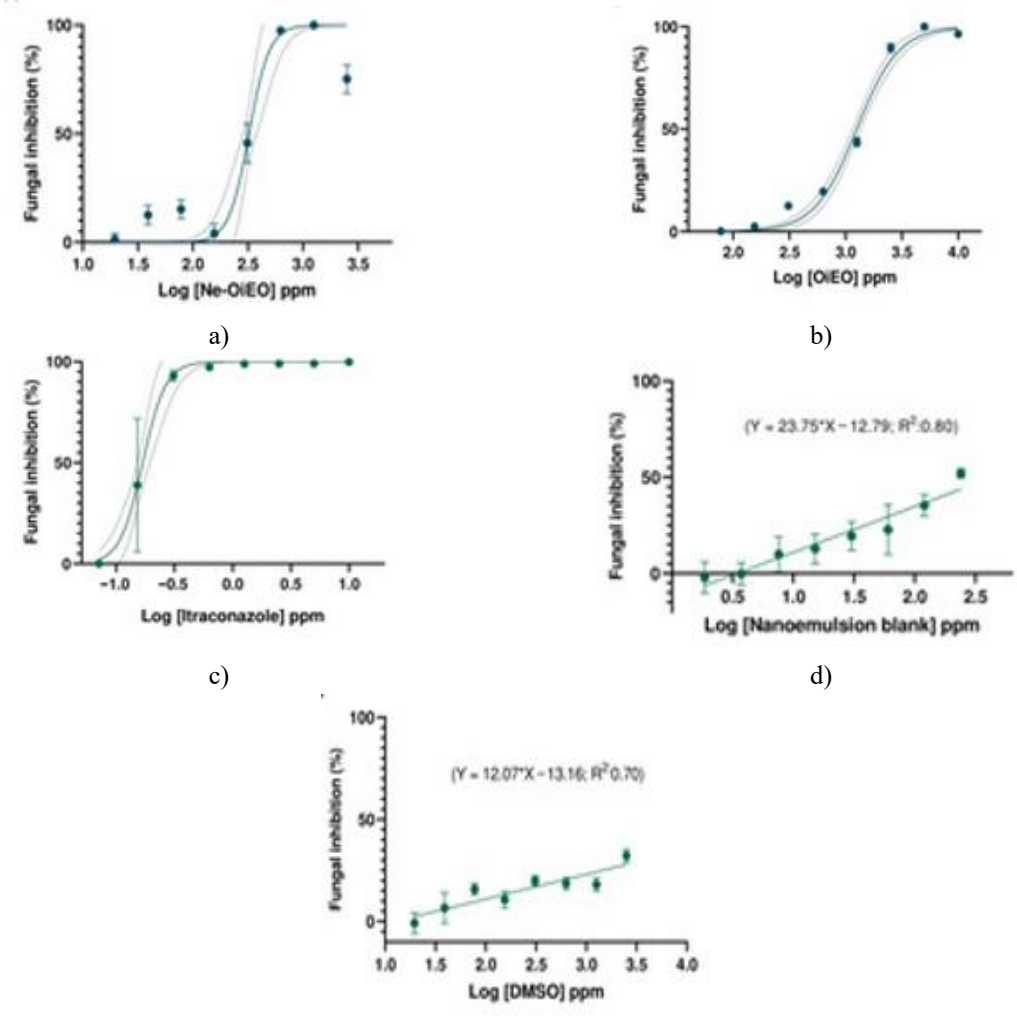

Figure 6. Dose–response relationships against *T. ethacetica*. Curves for *O. indecora* nanoemulsion (Ne-OiEO, (a), essential oil (OiEO, (b), and itraconazole (Itra, (c) were generated using nonlinear regression with normalized inhibition data. Confidence and prediction intervals (95%) are shown as dashed boundaries. Controls C-Ne (d) and Tween 80 (C-EO, (e) were modeled using linear regression. Each point represents the mean of three replicates, with standard deviation shown as error bars..

Fungistatic activity was evaluated using established qualitative and quantitative criteria. Both approaches indicated that Ne-OiEO inhibited *T. ethacetica* growth at 625 µg/mL, whereas OiEO required a higher concentration of 2500 µg/mL to achieve similar inhibition levels **(Table 5)**. The dose–response models showed strong goodness of fit, with R^2 values ranging from 0.70 to 0.96 and RMSE values between 19.14 and 5.6. IC50 analysis further demonstrated that the nanoemulsion achieved 50% growth inhibition at concentrations approximately three- to five-fold lower than the essential oil **(Table 5).** However, viability assays with resazurin, followed by subculturing onto BDA plates, confirmed that none of the treatments exhibited fungicidal activity against the tested pathogen.

Table 5. Antifungal activity of *O. indecora* nanoemulsion (Ne-OiEO) and essential oil (OiEO) against *Th. ethacetica*.

Treatment	Fungi	RMSE	R^2	95% IC_{50}	IC_{50} (µg/mL) [b]	MIC (µg/mL) [a]
Ne-OiEO	*T. ethacetica*	12.18	0.90	286.5–363.4	322.7	625
OiEO	*T. ethacetica*	5.65	0.98	1154–1355	1252.0	2500
Itraconazole *	*T. ethacetica*	10.4	0.92	0.1532–0.1890	0.1682	0.31

[a]: MIC = minimum inhibitory concentration determined by absence of visible growth (qualitative) or ≥ 80% inhibition (quantitative). [b]: IC50 = concentration (µg/mL) causing 50% inhibition; 95% CI = confidence intervals (non-overlapping indicates significant difference); IC50

derived from nonlinear regression of dose–response curves (three independent experiments); R^2 = coefficient of determination; RMSE = root mean square error. *Itraconazole used as positive control.

Fungal micromorphology

The development and structural differentiation of *T. ethacetica* under chemically contaminated nutrient conditions were evaluated using the poisoned culture medium method. As an anamorphic fungus, *T. ethacetica* produces multiple reproductive structures, including aleurioconidia and two endoconidial forms, designated primary and secondary conidia. Under standard growth conditions on BDA medium at 25 °C for 72 h, the fungus generated dark brown, thick-walled, elongated aleurioconidia (aC) averaging 12 × 6 µm. Its vegetative hyphae were smooth, hyaline, and measured approximately 3.87 µm in width. Secondary conidia appeared as light brown, ovoid, aseptate structures with dimensions of 7 × 4 µm. In addition, chains of cylindrical, transparent primary conidia (4.3 × 1.0 µm) were frequently observed.

Marked morphological interference was observed following exposure to itraconazole and *O. indecora* essential oil (OiEO) **(Figure 7a)**. At 10,000 µg/mL, OiEO severely impaired the formation of both aleurioconidia and primary conidia, while at 1250 µg/mL its effect was mainly restricted to suppression of primary conidia (pC). The nanoemulsion (Ne-OiEO) also altered fungal morphogenesis in a dose-dependent manner; at 2500 µg/mL it inhibited primary conidia development and reduced sporulation of aleurioconidia emerging from short lateral phialides (aC-F), whereas at 325 µg/mL the effect was less pronounced. In itraconazole-treated samples, secondary spores displaying narrowed vegetative tubes were detected, along with a noticeable reduction in mycelial expansion. Statistical analysis (ANOVA) demonstrated significant differences in secondary conidia size among all experimental groups ($P < 0.05$) **(Figure 7b)**. Because hyphal width data violated normality assumptions, the Kruskal–Wallis test was employed and confirmed significant treatment-related effects during fungal development ($P < 0.05$). Subsequent Dunn's post hoc analysis indicated that both Ne-OiEO (325 µg/mL) and OiEO (10,000 µg/mL) significantly reduced hyphal thickness relative to the untreated control. Even at the lowest concentration level tested (C4), neither Ne-OiEO nor OiEO fully inhibited aleurioconidia production; however, significant alterations in their dimensional profiles were still detected **(Figure 7d)**.

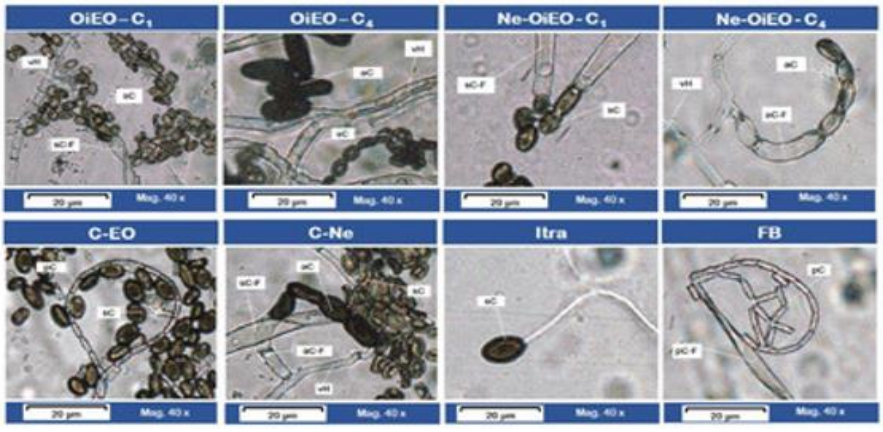

a)

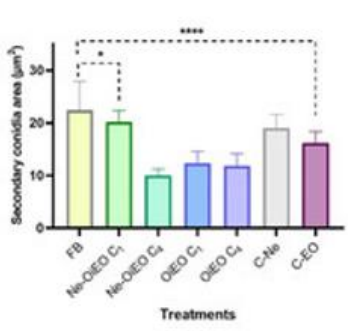

b)

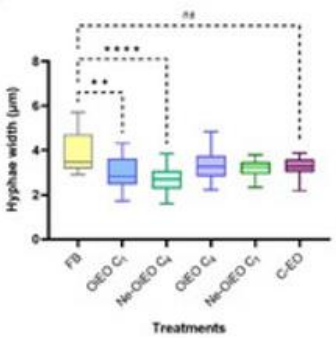

c)

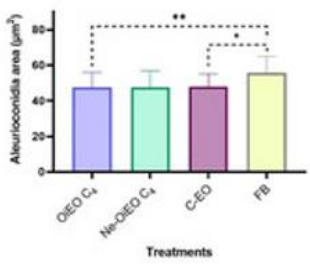

d)

Figure 7. Structural analysis of *T. ethacetica* following exposure to plant-based and chemical treatments via absorption assays. Ne-OiEO C1 and C4: *O. indecora* essential oil nanoemulsion at 2500 µg/mL and 325

µg/mL; OiEO C1 and C4: *O. indecora* essential oil at 10,000 µg/mL and 1250 µg/mL; C-Ne: blank nanoemulsion; C-EO: Tween 80; Itra: itraconazole; FB: fungal blank. (a) Composite micrographs depicting fungal structures, including vegetative hyphae (vH), aleurioconidia (aC), secondary conidia (sC), primary conidia (pC), secondary conidiophore phialides (sC-F), lateral aleurioconidia-forming phialides (f-aC), and apical phialides producing primary conidia (pC-F). (b) Quantification of secondary conidia area in *T. ethacetica*. Significant differences: * 0.0186; **** < 0.0001 (Dunnett's multiple comparisons test, $P < 0.05$). (c) Measurement of hyphal thickness in *T. ethacetica*; ns: not significant; significant differences ** 0.0037, **** < 0.0001 (Dunn's multiple comparisons test). (d) Measurement of aleurioconidia area in *T. ethacetica*; * 0.0129, ** 0.008 (Dunnett's multiple comparisons test, $P < 0.05$).

Previous literature has already described the essential oil obtained from *O. indecora* leaves. Studies conducted with specimens collected in the coastal sandbank region of Rio de Janeiro, consistent with the present work, confirmed sesquirosefuran as the predominant constituent of the leaf essential oil, with reported proportions ranging from 81.41% to 87.00%, as determined by GC-MS and NMR analyses [21, 22, 26, 33]. In contrast, samples collected from the Atlantic Forest of São Paulo showed a distinctly different chemical profile, dominated by bicyclogermacrene (29.79%), valerianol (15.12%), spathulenol (11.16%), and β-pinene (11.41%) [34]. It is important to emphasize that, in the current study, due to the absence of authentic reference standards for GC-MS confirmation, compound identification relied on mass spectral matching and retention index comparison with library databases; therefore, the assigned constituents should be regarded as putative identifications [35, 36].

Variation in plant metabolite profiles is widely recognized, as both biotic and abiotic environmental factors can significantly alter the qualitative and quantitative composition of secondary metabolites [37]. These interacting influences generate a high degree of metabolic flexibility that reflects plant ecological adaptation, but simultaneously complicate the standardization and reproducibility of plant-derived preparations [38]. Within this framework, the essential oil from *O. indecora* leaves collected in the Restinga de Jurubatiba National Park (Rio de Janeiro) appears to exhibit a relatively consistent chemical profile, as supported by both the present findings and previously published studies [22-26, 33].

Despite their biological potential, the practical use of essential oils remains limited due to intrinsic physicochemical characteristics such as high volatility and strong lipophilicity, which hinder formulation development for pharmaceutical and agricultural applications [19, 39]. As a result, nanoemulsification has become a widely explored strategy for improving the delivery of essential oils [40]. This approach enhances application performance by improving dispersion in aqueous media, and nanoemulsified systems have also been shown to increase biological activity through improved bioavailability, membrane permeation, and absorption efficiency [19].

For a dispersed colloidal system to be classified as a nanoemulsion, it must generally exhibit droplet diameters between 20 and 200 nm and a polydispersity index lower than 0.3, indicating a relatively uniform (monodisperse) distribution [41]. In this study, the experimentally obtained nanoformulations displayed droplet sizes ranging from 72 to 198.5 nm and PdI values between 0.045 and 0.287, which collectively fall within an acceptable nanometric range, confirming successful nanoemulsion formation. In addition, the formulations exhibited characteristic macroscopic features, including a bluish opalescence, while those with lower essential oil content appeared more translucent [42].

The outcomes of the factorial design are consistent with earlier reports demonstrating that reduced oil-phase concentrations combined with higher surfactant levels decrease interfacial tension and improve surface coverage, ultimately producing smaller droplets and narrower size distributions [43]. Similarly, the role of sonication amplitude aligns with established principles of ultrasonic emulsification, in which increased energy input enhances droplet disruption and reduces the mean particle size [44]. Overall, these results corroborate the literature and indicate that optimal nanoemulsion properties are achieved using lower oil content, higher surfactant concentrations, and optimized sonication energy, which together favor reduced droplet size and acceptable polydispersity [45].

Stability assessment of Ne-OiEO revealed that formulations stored for 90 days at room temperature (25 °C) and under refrigeration (8 °C) maintained physical integrity without evident destabilization. Conversely, storage at 42 °C induced instability, likely due to partial dehydration of the hydrophilic polyethylene oxide (PEO) segments of Pluronic-L64 at the droplet interface, thereby weakening steric stabilization [18]. Under elevated-temperature conditions, enhanced Brownian motion, combined with reduced continuous-phase viscosity, promoted increased

droplet collisions and accelerated creaming, in agreement with Stokes' law [46]. Additionally, higher temperatures facilitate Ostwald ripening, in which molecular diffusion from smaller droplets to larger ones promotes particle growth and phase separation [47]. Collectively, these mechanisms reflect the inherent thermodynamic instability of nanoemulsions and highlight the effectiveness of Pluronic L64 in stabilizing *O. indecora* essential oil systems at lower temperatures.

Both *O. indecora* essential oil (OiEO) derived from leaves and its nanoemulsion (Ne-OiEO) exhibited antibacterial and bactericidal activity against Gram-positive bacteria at concentrations between 1 and 2 mg/mL. Although no previous studies have reported antibacterial activity specifically for *O. indecora* essential oil, similar inhibitory ranges have been documented for essential oils from other *Ocotea* species against bacterial strains [48-51]. In the present study, nanoemulsification did not significantly enhance growth inhibition but did improve bactericidal efficacy against *S. aureus* ATCC 25923. This suggests that encapsulation within the nanoemulsion matrix likely improved dispersion and bioavailability of lipophilic compounds without altering the minimum inhibitory threshold during the 24-hour exposure period, possibly due to controlled or delayed release behavior typical of nanostructured delivery systems [20].

A key outcome of the present investigation was the notable increase in antifungal potency following nanoemulsification. The Ne-OiEO formulation demonstrated fungistatic activity at 625 µg/mL, a concentration substantially lower than that required for the non-formulated essential oil (MIC = 2500 µg/mL), confirming that nanoemulsion processing enhances antifungal performance. As a benchmark compound, itraconazole exhibited an MIC of 0.31 µg/mL, corresponding to approximately a 2016-fold difference in potency relative to the nanoemulsion. Similar enhancements in antifungal efficacy have been reported for nanoformulated essential oils derived from *Myristica fragrans*, *Bunium persicum*, and *Zanthoxylum alatum*, which also improved inhibition of *A. flavus* and reduced aflatoxin B1 production [9]. Nevertheless, this behavior is not universally consistent across studies. For instance, Cruz *et al*. [52] observed that a nanoemulsion of *Lippia gracilis* showed reduced antifungal activity, with higher MIC values (600 µg/mL) against Thielaviopsis paradoxa than its essential oil (230–260 µg/mL). Such contradictory evidence indicates that nanoemulsion effects are strongly system-specific, depending on oil composition, the target microorganism, the methodological design, and the release dynamics of encapsulated compounds [53, 54].

Antimicrobial activity in plant extracts is typically dominated by the principal constituent, in this case sesquirosefuran; however, the involvement of secondary metabolites such as spathulenol, dendrolasin, and β-farnesene should also be considered [55]. Oils enriched in spathulenol have repeatedly demonstrated broad antibacterial and antifungal properties, reinforcing its role as an active sesquiterpene component [56, 57]. Therefore, the overall antifungal and antibacterial effects observed here may arise from combined or synergistic interactions among multiple constituents rather than a single dominant compound.

The morphological traits of *T. ethacetica* observed in this study closely correspond to earlier descriptions by Borges *et al*. [7], Nascimento *et al*. [8], and Mbenoun *et al*. [32], who studied isolates from pineapple and cocoa in Cameroon and from sugarcane and oil palm in northern Brazil. Conidial structures are central to fungal survival, dissemination, and pathogenicity, making their study essential for disease monitoring and integrated crop protection strategies [7, 8, 32]. Although *O. indecora* essential oil exhibited a fungistatic effect, the present results indicate that once internalized by *T. ethacetica*, it disrupts mycelial expansion, interferes with nutrient uptake, and alters hyphal development and propagule formation. In addition, OiEO affected sporulation behavior. At the highest concentration tested, both formulations reduced the size of secondary conidia, which are involved in disease transmission. Also, they suppressed the development of resistant structures, such as aleurioconidia and primary conidia. This suppression is particularly relevant because aleurioconidia contribute to the pathogen's long-term survival in soil, allowing persistence for up to 16 months under adverse conditions [58]. Overall, the data support the potential of *O. indecora* essential oil and its nanoemulsion as promising natural antimicrobial candidates.

Conclusion

This study investigated the antimicrobial potential of *O. indecora* essential oil alongside its nanoemulsified form. Optimization using a factorial experimental design revealed that formulations with a reduced oil fraction, increased surfactant concentration, and higher sonication intensity yielded more stable nanoscale dispersions.

In antibacterial assays, nanoemulsification produced only a limited improvement in growth inhibition; however, it enhanced bactericidal activity against *S. aureus*. In contrast, antifungal evaluation demonstrated a clearer benefit, with the nanoemulsion achieving lower MIC values against *T. ethacetica* compared to the unformulated oil. Both formulations also induced clear morphological disruptions in fungal structures, including impaired hyphal integrity and altered sporulation processes.
Overall, the findings indicate that *O. indecora* essential oil and its nanoemulsion represent promising bioactive systems with potential applications in antimicrobial development, supporting further exploration as natural alternatives in medical and agricultural contexts.

Acknowledgments: The authors express their gratitude to UNIMICRO/UFRJ for the scientific support provided in the transmission electron microscopy (TEM) analyses, and to LCAN/FF/UFF for assistance with the gas chromatography (GC) analyses. The authors also extend special thanks to Mauricio Afonso Vericimo, coordinator of the Laboratory of Immunology of Infectious and Granulomatous Diseases (LIGID-IB-UFF), and to Sabrina Calil Elias, coordinator of the Laboratory of Pharmacology (FF-UFF), for making their facilities available for the antifungal assays.

Conflict of Interest: None

Financial Support: This research grant was funded by the National Council for Scientific and Technological Development (CNPq, Grant No. 304179/2021-3), the Coordenação de Aperfeiçoamento de Pessoal de Nível Superior (CAPES, Grant No. 001), and Fundação de Amparo à Pesquisa do Estado do Rio de Janiro (FAPERJ) via Grants E-26/200.161/2025, E-26/200.162/2025 (304867), E-26/210.598/2023 (285944), and E-26/200.915/2022 (268191).

Ethics Statement: None

References

1. Salam MA, Al-Amin MY, Salam MT, Pawar JS, Akhter N, Rabaan AA, et al. Antimicrobial resistance: a growing serious threat for global public health. Healthcare. 2023;11:1946.
2. Murni IK, Duke T, Kinney S, Daley AJ, Wirawan MT, Soenarto Y. Risk factors for healthcare-associated infection among children in a low- and middle-income country. BMC Infect Dis. 2022;22:1-7.
3. Hyde KD, Baldrian P, Chen Y, Thilini Chethana KW, De Hoog S, Doilom M, et al. Current trends, limitations and future research in the fungi. Fungal Divers. 2024;125:1-71.
4. Eskola M, Kos G, Elliott CT, Hajšlová J, Mayar S, Krska R. Worldwide contamination of food-crops with mycotoxins: validity of the widely cited 'FAO estimate' of 25%. Crit Rev Food Sci Nutr. 2020;60:2773-89.
5. van Rhijn N, Rhodes J. Evolution of antifungal resistance in the environment. Nat Microbiol. 2025;10:1804-15.
6. Yarahmadi A, Najafiyan H, Yousefi MH, Khosravi E, Shabani E, Afkhami H, et al. Beyond antibiotics: exploring multifaceted approaches to combat bacterial resistance in the modern era: a comprehensive review. Front Cell Infect Microbiol. 2025;15:1493915.
7. Borges AF, de Alcântara Neto F, da Silva Matos K, Júnior JEAB, Júnior NSM, Moreira SI, et al. Thielaviopsis ethacetica the etiological agent of sugarcane pineapple sett rot disease in Brazil. Trop Plant Pathol. 2019;44:460-7.
8. Nascimento SMCD, Nakasone AK, Neto CFO, Alves KF, Sobrinho RSA, Conceição SS, et al. Patogenicidade e caracterização de Thielaviopsis ethacetica em palma de óleo. Summa Phytopathol. 2020;46:236-41.
9. Yadav A, Kumar A, Singh PP, Prakash B. Pesticidal efficacy, mode of action and safety limits profile of essential oils based nanoformulation against Callosobruchus chinensis and Aspergillus flavus. Pestic Biochem Physiol. 2021;175:104813.
10. Angane M, Swift S, Huang K, Butts CA, Quek SY. Essential oils and their major components: an updated review on antimicrobial activities, mechanism of action and their potential application in the food industry. Foods. 2022;11:464.

11. Singha B, Singh V, Soni V. Alternative therapeutics to control antimicrobial resistance: a general perspective. Front Drug Discov. 2024;4:1385460.
12. Wan NF, Fu L, Dainese M, Kiær LP, Hu YQ, Xin F, et al. Pesticides have negative effects on non-target organisms. Nat Commun. 2025;16:1-16.
13. Beyuo J, Sackey LNA, Yeboah C, Kayoung PY, Koudadje D. The implications of pesticide residue in food crops on human health: a critical review. Discov Agric. 2024;2:1-19.
14. Gyawali R, Ibrahim SA. Natural products as antimicrobial agents. Food Control. 2014;46:412-29.
15. Singh BK, Tiwari S, Dubey NK. Essential oils and their nanoformulations as green preservatives to boost food safety against mycotoxin contamination of food commodities: a review. J Sci Food Agric. 2021;101:4879-90.
16. Baptista-Silva S, Borges S, Ramos OL, Pintado M, Sarmento B. The progress of essential oils as potential therapeutic agents: a review. J Essent Oil Res. 2020;32:279-95.
17. Mutlu-Ingok A, Devecioglu D, Dikmetas DN, Karbancioglu-Guler F, Capanoglu E. Antibacterial, antifungal, antimycotoxigenic, and antioxidant activities of essential oils: an updated review. Molecules. 2020;25:4711.
18. Marhamati M, Ranjbar G, Rezaie M. Effects of emulsifiers on the physicochemical stability of oil-in-water nanoemulsions: a critical review. J Mol Liq. 2021;340:117218.
19. Vikal A, Maurya R, Patel P, Das Kurmi B. Nanoemulsion technology in oral drug delivery: a path to enhanced solubility and bioavailability. Curr Pharm Des. 2025;31:2881-96.
20. Garcia CR, Malik MH, Biswas S, Tam VH, Rumbaugh KP, Li W, et al. Nanoemulsion delivery systems for enhanced efficacy of antimicrobials and essential oils. Biomater Sci. 2022;10:633-53.
21. Figueiredo A, Nascimento LM, Lopes LG, Giglioti R, Albuquerque RDDG, Santos MG, et al. First report of the effect of Ocotea elegans essential oil on Rhipicephalus (Boophilus) microplus. Vet Parasitol. 2018;252:131-6.
22. Toledo PFS, da Cruz Araujo SH, Mantilla Afanador JG, Silva ACF, Machado FP, Rocha LM, et al. Potential of Ocotea indecora essential oil for controlling Drosophila suzukii: molecular predictions for toxicity and selectivity to beneficial arthropods. Neotrop Entomol. 2024;53:189-99.
23. Nascimento LM, Apolinario R, Machado FP, Correa AL, Caldas GR, Ruppelt BM, et al. Effects of nanoemulsion and essential oil from the leaves of Ocotea elegans against Dysdercus peruvianus. Res Soc Dev. 2020;9:e909108424.
24. Machado FP, Folly D, Salas Enriquez JJ, Mello CB, Esteves R, Araújo RS, et al. Nanoemulsion of Ocotea indecora (Shott) Mez essential oil: larvicidal effects against Aedes aegypti. Ind Crops Prod. 2023;192:116031.
25. Pinto LDA, Machado FP, Esteves R, Farias VM, Köptcke FBN, Ricci-Junior E, et al. Characterization and inhibitory effects of essential oil and nanoemulsion from Ocotea indecora (Shott) Mez in Aspergillus species. Molecules. 2023;28:3437.
26. Machado FP, Diniz-dos-Santos AC, de Queiroz LN, Fernandes CP, Rocha L, Robbs BK. Cell death by apoptosis induced by Ocotea indecora (Schott) Mez essential oil in different cancer cell lines. Nat Prod Res. 2024. Epub ahead of print.
27. Adams RP. Identification of essential oil components by gas chromatography/mass spectroscopy. 4th ed. Carol Stream (IL): Allured Publishing; 2007.
28. El-Sayed A. The Pherobase: database of pheromones and semiochemicals [Internet]. Available from: https://www.pherobase.com/
29. de Siqueira LBDO, dos Santos Matos AP, da Silva Cardoso V, Villanova JCO, Guimarães BDCLR, de Santos EP, et al. Clove oil nanoemulsion showed potent inhibitory effect against Candida spp. Nanotechnology. 2019;30:425101.
30. Souza DP, Pimentel RBQ, Santos AS, Albuquerque PM, Fernandes AV, Junior SD, et al. Fungicidal properties and insights on the mechanisms of the action of volatile oils from Amazonian Aniba trees. Ind Crops Prod. 2020;143:111914.
31. Rasband WS. ImageJ [Internet]. Bethesda (MD): U.S. National Institutes of Health; 2018. Available from: https://imagej.net/ij/
32. Mbenoun M, de Beer ZW, Wingfield MJ, Wingfield BD, Roux J. Reconsidering species boundaries in the Ceratocystis paradoxa complex, including a new species from oil palm and cacao in Cameroon. Mycologia. 2014;106:757-84.

33. Paiva Machado F, da Silva Rangel L, Nunes Farias Gomes K, Albuquerque Dos Santos JA, Xavier Faria R, Santos MG, et al. Potential of Ocotea indecora (Schott) Mez essential oil nanoemulsion in schistosomiasis control: molluscicidal effects. Exp Parasitol. 2024;259:108717.
34. Gonçalves RDA, Pinheiro AB, De Oliveira MA, Nascimento RTD, Rosalem PF, Garcia VL, et al. Anatomical characters and chemical profile of leaves of three species in Lauraceae family. Rev Bras Farmacogn. 2018;28:1-8.
35. van Den Dool H, Kratz PD. A generalization of the retention index system including linear temperature programmed gas-liquid partition chromatography. J Chromatogr A. 1963;11:463-71.
36. Sadgrove NJ, Padilla-González GF, Phumthum M. Fundamental chemistry of essential oils and volatile organic compounds, methods of analysis and authentication. Plants. 2022;11:789.
37. Abdelmohsen UR, Elmaidomy AH. Exploring the therapeutic potential of essential oils: a review of composition and influencing factors. Front Nat Prod. 2025;4:1490511.
38. Wu F, Chen Y, Gao M, Li W, Zhao Y, Wang Y. An updated review on essential oils from Lauraceae plants: chemical composition and genetic characteristics of biosynthesis. Int J Mol Sci. 2025;26:5690.
39. Kumar A, Kanwar R, Mehta SK. Nanoemulsion as an effective delivery vehicle for essential oils: properties, formulation methods, destabilizing mechanisms and applications in agri-food sector. Next Nanotechnol. 2025;7:100096.
40. Barradas TN, de Holanda e Silva KG. Nanoemulsions of essential oils to improve solubility, stability and permeability: a review. Environ Chem Lett. 2021;19:1153-71.
41. McClements DJ, Jafari SM. General aspects of nanoemulsions and their formulation. In: Jafari SM, editor. Nanoemulsions: formulation, applications, and characterization. Amsterdam: Elsevier; 2018. p. 3-20.
42. Preeti, Sambhakar S, Malik R, Bhatia S, Al Harrasi A, Rani C, et al. Nanoemulsion: an emerging novel technology for improving the bioavailability of drugs. Scientifica (Cairo). 2023;2023:6640103.
43. Mushtaq A, Mohd Wani S, Malik AR, Gull A, Ramniwas S, Ahmad Nayik G, et al. Recent insights into nanoemulsions: their preparation, properties and applications. Food Chem X. 2023;18:100684.
44. O'Sullivan JJ, Park M, Beevers J, Greenwood RW, Norton IT. Applications of ultrasound for the functional modification of proteins and nanoemulsion formation: a review. Food Hydrocoll. 2017;71:299-310.
45. Alderees F, Akter S, Mereddy R, Sultanbawa Y. Formulation, characterization, and stability of food grade oil-in-water nanoemulsions of essential oils of Tasmannia lanceolata, Backhousia citriodora and Syzygium anisatum. J Food Saf. 2022;42:e13001.
46. Soni M, Yadav A, Maurya A, Das S, Dubey NK, Dwivedy AK. Advances in designing essential oil nanoformulations: an integrative approach to mathematical modeling with potential application in food preservation. Foods. 2023;12:4017.
47. Guo Y, Zhang X, Wang X, Zhang L, Xu Z, Sun D. Nanoemulsions stable against Ostwald ripening. Langmuir. 2024;40:1364-72.
48. Nomentsoa RZ, Judicael RL, Ranjàna RH, Manampisoa RA, Doll RDA, Louis JV. Chemical composition and antibacterial activities of the essential oils from Ocotea zahamenensis Van Der Werff (Lauraceae). GSC Biol Pharm Sci. 2021;16:115-25.
49. Betim FCM, de Oliveira CF, de Souza AM, Szabo EM, Zanin SMW, Miguel OG, et al. Ocotea nutans (Nees) Mez (Lauraceae): chemical composition, antioxidant capacity and biological properties of essential oil. J Pharm Sci. 2019;55:18284.
50. Passos BG, de Albuquerque RDDG, Muñoz-Acevedo A, Echeverria J, Llaure-Mora AM, Ganoza-Yupanqui ML, et al. Essential oils from Ocotea species: chemical variety, biological activities and geographic availability. Fitoterapia. 2022;156:105065.
51. de Almeida RS, Ribeiro-Filho J, Freitas PR, de Araújo ACJ, dos Santos EL, Tintino SR, et al. Enhancement of the antibiotic activity mediated by the essential oil of Ocotea odorifera (Vell.) Rowher and safrole association. J Infect Public Health. 2022;15:373-7.
52. Cruz EMO, Mendonça MC, Blank AF, Sampaio TS, Pinto JAO, Gagliardi PR, et al. Lippia gracilis Schauer essential oil nanoformulation prototype for the control of Thielaviopis paradoxa. Ind Crops Prod. 2018;117:245-51.
53. dos Santos RD, Matos BN, Freire DO, da Silva FS, do Prado BA, Gomes KO, et al. Chemical characterization and antimicrobial activity of essential oils and nanoemulsions of Eugenia uniflora and Psidium guajava. Antibiotics (Basel). 2025;14:93.

54. Monteiro EDS, da Silva FS, Gomes KO, Prado BAD, dos Santos RD, da Camara CAG, et al. Characterization and determination of the antibacterial activity of Baccharis dracunculifolia essential-oil nanoemulsions. Antibiotics (Basel). 2023;12:1677.
55. Noshirvani N. Essential oils as natural food preservatives: special emphasis on antimicrobial and antioxidant activities. J Food Qual. 2024;2024:5807281.
56. Barboucha G, Rahim N, Boulebd H, Bramki A, Andolfi A, Salvatore MM, et al. Chemical composition, in silico investigations and evaluation of antifungal, antibacterial, insecticidal and repellent activities of Eucalyptus camaldulensis Dehn. leaf essential oil from Algeria. Plants. 2024;13:3229.
57. Freires IA, Denny C, Benso B, De Alencar SM, Rosalen PL. Antibacterial activity of essential oils and their isolated constituents against cariogenic bacteria: a systematic review. Molecules. 2015;20:7329-58.
58. Aparecido CC, Azania CAM. Podridão abacaxi em cana-de-açúcar. São Paulo: Instituto Biológico; 2012. (Comunicado Técnico 175).